

1 Water Distribution-Transportation Interface Connectivity

2 Responding to Urban Geospatial Morphology

3 Noha Abdel-Mottaleb¹ and Qiong Zhang²

4 ABSTRACT

5 Water distribution and transportation systems are geospatially co-located, forming a net-
6 work of connections. This network of connections is referred to as an *interface network*. Inves-
7 tigation of interface network connectivity can help understand and minimize failure propaga-
8 tion from water to transportation systems. Water distribution–transportation interface networks
9 consist of nodes, which can be either pipes or roads, and edges, which represent the geospatial
10 co-location of a pipe and road. The purpose of this study is twofold: to topologically represent
11 geospatial co-location by characterizing the connectivity of water distribution– transportation
12 interface networks for multiple cities, and to identify the nodal attributes that are most pre-
13 dictive of a given connectivity profile. A total of forty interface networks from eight cities of
14 varying geospatial morphology are extracted and analyzed using network analysis and machine
15 learning. Using network analysis, we investigate if the topological connectivity between water
16 and transportation is consistent across different cities. Then we use a random forest model to
17 ascertain which nodal attributes may have predictive power to identify the connectivity cluster
18 of the city to which a node belongs. Results indicate that cities of different geospatial mor-
19 phology may vary in their interface network connectivity, and average shortest path length of

¹Ph.D. Student, Department of Civil and Environmental Engineering, University of South Florida 4202 E. Fowler Ave., ENB 118 Tampa, Florida, 33620. Email: nohaa@mail.usf.edu

²Associate Professor, Department of Civil and Environmental Engineering, University of South Florida 4202 E. Fowler Ave., ENB 118 Tampa, Florida, 33620. Email: qiongzhang@usf.edu

20 a given node is the major nodal feature contributing to a given city's interface network con-
21 nectivity. These findings hold implications for urban planning and water distribution design to
22 mitigate potential cascading failures.

23 **Keywords:** water distribution networks, interdependency, transportation networks,
24 urban morphology, complexity

25 **INTRODUCTION**

26 Water distribution and transportation systems are both critical infrastructures, cru-
27 cial and integral to the functioning of cities. All people need access to water and mo-
28 bility from and to different locations in cities. In fact, a lack of performance of these
29 two types of infrastructures can even be life-threatening. To compound the complexity
30 of these two infrastructure systems, they cannot be analyzed independently because
31 the failure of water distribution networks (e.g. pipe and main breaks) has a direct im-
32 pact on transportation networks as has been illustrated by traffic disruptions and their
33 subsequent socio-economic impacts (Reed 2017; Chen et al. 2018) and as alluded to in
34 urban design and architecture literature (Alexander 1977; Ahern 2011; Meerow et al.
35 2016). Further, in addressing or repairing component failures within water distribu-
36 tion, an impact to transportation occurs by way of accessing the underground piping
37 which is often located beneath roads (Mair et al. 2017). This type of interdependency
38 between water distribution and transportation networks, due to co-location, is referred
39 to as geospatial interdependency.

40 There are many different models to study interdependent infrastructures, depending
41 on the purpose, systems' specifications, and data availability. Some of the more com-
42 mon approaches include: agent-based models, inoperability input output models, sys-
43 tems dynamics, probabilistic methods, multi-objective optimization, network-based
44 approaches, and combinations thereof (Ouyang 2014; Johansen and Tien 2018). Network-
45 based approaches include both structural (i.e. as a snapshot of topology) and dynamics
46 on the network (defining stress/failure states and involving stress/failure propagation

47 probabilities). Further, the coupled networks can be modeled in a variety of ways us-
48 ing a network approach. The choice of model and analysis is in part influenced by
49 data availability/understanding of the system, and also the type of interdependency
50 between the infrastructures, as interdependency can be physical, geo-spatial (i.e. co-
51 location/proximity), cyber, or logical (Gillette et al. 2002; Rinaldi et al. 2001). Be-
52 cause network science is an interdisciplinary field, variations of the same method and
53 type of multi-layer networks have been called by different names in the literature (e.g.
54 influence model, deterministic/probabilistic Bayesian network, coupled network, in-
55 terlinked network, in addition to multi-layer/multiplex). Multi-layer networks are of-
56 ten used to study the dynamics on interdependent networks, where each infrastructure
57 network layer has its own properties and connections (and thus cascading failure dy-
58 namics), in addition to a layer of distinct connections between the two layers (Kivelä
59 et al. 2014; Boccaletti et al. 2014; Bianconi 2018). Researchers have used both real,
60 virtual, or generic network data to construct these multi-layer network models. Find-
61 ings often show that what constitutes a robust network from analyzing it alone, is
62 different when considering coupled infrastructures together (i.e. interconnected infras-
63 tructure networks each can respond uniquely to external events, internal failures, and
64 operation errors) (Haimes et al. 2005; Winkler et al. 2011; Ouyang et al. 2012; Casal-
65 icchio and Galli 2008; Rinaldi et al. 2001). Abdel-Mottaleb et al. (2019) have also
66 previously shown that whether or not considering interdependency in management de-
67 cisions can be dependent on the size/magnitude of failures between water distribution
68 pipe network and transportation road network. Due to the coupling between infras-
69 tructures, studies have treated two (or in rare cases more) networks together as multi-
70 layer/multiplex networks, where dependencies are assumed to be either unidirectional
71 (only one infrastructure depends on the other) or bidirectional (both infrastructures de-
72 pend on each other in some way) (Dueñas-Osorio et al. 2007; Svendsen and Wolthusen
73 2007; Ouyang and Dueñas-Osorio 2011a; Ouyang and Dueñas-Osorio 2011b; Das

et al. 2014; Danziger et al. 2016; Wang et al. 2019; Buldyrev et al. 2010; Korkali et al. 2017; Guidotti et al. 2016; Rahnamay-Naeini and Hayat 2016; Johansen and Tien 2018; Abdel-Mottaleb et al. 2019). Most research on interdependent infrastructures has focused on the failure dynamics of the coupled infrastructure layers, without an analysis of the structure of the interface (i.e. the network consisting of components that directly influence each other from both infrastructure layers) between them. While Winkler et al. (2011) did study the structure of the potable water-power interface for a case study, the interdependency between the two infrastructures is more functional than it is geo-spatial (or due to co-location). Whereas the interdependency between water distribution pipes and transportation roads is heavily co-location based. Furthermore, there have not been studies on how interface structure may vary for different urban development schemes (i.e. geo-spatial morphology). To address these gaps, this study characterizes structural network properties of water pipe-road interface (a network of connections) instead of simulating dynamics on a multi-layer network. We start with a multi-layer network consisting of pipes and roads, but only the pipes and roads that are co-located are extracted to generate a network of the connections of the two layers. We seek to find if the structure of the interdependent linkages between water and transportation is some sort of universal property, independent of a city's geo-spatial layout or if it can vary for cities that developed in different patterns. To date no study has characterised the complex network structure of the *interface* between water distribution pipes and transportation road networks. The interface network, similar to the definition in Winkler et al. (2011) and Ouyang and Dueñas-Osorio (2011a), refers to the network of connections between water distribution and transportation. Nodes in the interface represent infrastructure components from either water distribution or transportation (i.e. pipes or roads) and edges represent potential failure propagation, due to geospatial interdependence.

The water-transportation interface as a logical network is derived from the physical wa-

101 ter distribution infrastructure and surface transportation infrastructure. The topology
102 and structure of a given infrastructure network is constrained by geospatial boundaries.
103 Thus, geospatial morphology is a contributor to the form an infrastructure network
104 takes (Louf and Barthelemy 2014). Gastner and Newman (2004) identified geography
105 as a main driver of distribution networks' overall layout and shape. Water distribution
106 networks, specifically, are spatially constrained by the environments in which they are
107 located due to both geology and spatial impediments. Hence, they often trace the same
108 path as other utility networks such as transportation, urban drainage (sanitary sewer
109 and stormwater), and power, which also suffer the same geospatial constraints (Zischg
110 et al. 2017; Yang et al. 2017). Spatial impediments are not only a result of a city's ge-
111 ography, but its morphology (i.e. how it's form developed and continues to do so over
112 time). The layout of a city's infrastructure networks evolves as a spatial and temporal
113 event, in so much as it is driven yet constrained by a city's morphology. This evolution-
114 ary morphologic phenomenon yields distinct urban forms throughout the world. Porta
115 et al. (2006) identified six general city forms in their research on networks in urban
116 design: medieval, grid-iron, modernist, baroque, mixed, and lollipop (post-war, low
117 density sprawled suburbs). Different urban forms cities may take, and the properties
118 or characteristics of each, have been identified and studied by (Boeing 2017; Boeing
119 2019; Alexander 1977)

120 In this vain, cities with different urban forms around the world will have infrastructure
121 networks with varying layout. However, this does not guarantee that infrastructure
122 interfaces (i.e. network of connections between two or more infrastructure networks)
123 vary in their network characteristics. Given that water distribution and transportation
124 systems are as interdependent as they are regarding potential failure propagation from
125 water to transportation, it is of importance to investigate structural properties of the
126 interface network between them. Network structure is integral to understanding inter-
127 dependent and complex infrastructure systems; information such as connectivity can

128 be extrapolated from structure. Similar to the limitations imposed on entire cities' layout
129 and shape by geospatial form, infrastructure networks' efficiency (i.e. resistance to
130 failure) has been linked to structural properties in both individual and interdependent
131 infrastructures (Winkler et al. 2011; Porta et al. 2006).

132 Within network analysis, observations can be made at different, often compartmentalized
133 into three scales: micro, community, and macro (Soundarajan et al. 2014).
134 Soundarajan et al. (2014) classified the different scales based on operation level. For
135 example, micro scale refers to nodal measurements (i.e. measurements of the constituent
136 parts), while macro refers to network wide, global measures. Community scale refers to the
137 nodal neighborhood level. Complex systems cannot be understood by solely examining and
138 analyzing their constituent parts – or micro-scale analyses; they are defined more by their internal
139 relationships than by their constituent parts. Network connectivity quantitatively captures the extent of
140 relationships between constituent parts (i.e. nodes) of a network. Moreover, using a combination of observation
141 across scales, patterns can be found that relate micro and community scale measures to
142 macro- scale phenomena, and thus allow for predictions to be made regarding network-
143 wide properties from measured nodal characteristics. This is relevant to infrastructure
144 operation and management, because decisions and design are enacted on a component-
145 level, with aim of yielding particular network-wide or global characteristics. For ex-
146 ample, the work of Porta et al. (2006) showed that micro-scale streets in transportation
147 networks that were locally efficient yielded an overall transportation network that also
148 tended towards global efficiency. Also in the case of water distribution-transportation
149 interfaces, a decrease in failure propagation between the two networks is a desirable
150 network-wide goal. To understand such network structure properties, complex network
151 theory and modeling has been applied.

153 Complex network analysis has been used to study the structure of transportation road
154 networks (Louf and Barthelemy 2014; Boeing 2017; Zhang et al. 2015) and water dis-

155 tribution networks (Yazdani and Jeffrey 2010; Yazdani and Jeffrey 2012; Giustolisi
156 et al. 2017; Giudicianni et al. 2018; Di Nardo et al. 2018). Such an analysis has not
157 been conducted for the water distribution-transportation interface.

158 To address this limitation, this study seeks to investigate and characterize connectiv-
159 ity of the interface between water and transportation networks among different cities,
160 which may be indicative of potential failure propagation from water distribution to
161 transportation. Then, this study uses that knowledge to identify micro-scale features
162 that best predict macro-scale network wide connectivity of the interface between water
163 and transportation networks. To this aim, network analysis is fortified with machine
164 learning to be able to identify patterns emerging from local (micro-scale) features into
165 global (network-wide) properties.

166 **METHODOLOGY**

167 In this study, higher network connectivity between water distribution and trans-
168 portation infrastructure networks is assumed to indicate higher propensity for failure
169 propagation. Due to the inevitable co-location of water distribution and transportation
170 road networks, it was not clear if the interface network between the two infrastructures
171 could have different connectivity for a city in which the infrastructures were located.
172 To investigate this, several different measures of global, network-wide connectivity are
173 used. Four topological connectivity metrics are computed for 5 samples of a set of 8
174 cities. Five samples are selected for statistical robustness, to account for the variability
175 driven by different possible layouts for a water distribution network within a single
176 city.

177 The workflow of the methodology is delineated in Figure 1. The study begins with the
178 selection of cities and results in assessment of network-wide interface connectivity and
179 identification of a nodal predictor that predicts interface connectivity.

FIG. 1

180 **City Selection**

181 City selection ensures the analysis of a representative set of geospatial morpholog-
182 ical conditions constraining water distribution networks' layout. A literature review is
183 conducted to choose cities that are identified as differing in age and geomorphology,
184 and also to allow for extending research and knowledge that is already present (i.e.
185 to deepen the body of knowledge) (Alexander 1977; Boeing 2017; Porta et al. 2006).
186 Within the urban planning and transportation body of literature, city shapes are distin-
187 guished: older and circular; newer grid like; coastal, linear, tree like; mix of dense old
188 circular city and sparser extensions, thereby allowing the selection of eight cities of
189 varying spatial geometry and evolutionary development. The eight selected cities are:
190 Boston, Chicago, Portland, and Atlanta within the USA; Rome, Italy; Paris, France;
191 Dubai, UAE; and Alexandria, Egypt.

192 Maps of the studied cities are shown in Figure 2. Polar histograms of street orienta-
193 tions are inlaid in the maps using the opensource Mapbox tool by Agafonkin (2018)
194 with map data from (Mapbox 2018; Contributors 2012). Though street orientations
195 do not completely represent the complexity of the studied urban areas' layouts, they
196 highlight some of the significant differences in their development patterns. For ex-
197 ample, Portland is the most "grid-like" city, and that is shown in its polar histogram
198 because the rainbow bars are concentrated along four directions. However, Rome is
199 the most "circularly" laid out, as can be seen from its histogram indicating that streets
200 are oriented in all directions.

FIG. 2

201 **Data Collection**

202 Transportation road network data for each respective city is extracted from Open-
203 streetmap (Contributors 2012). Five water distribution network models for each city of
204 study are generated using an open source virtual water distribution network generator
205 (DynaVIBe) developed by Sitzenfrei et al. (2010). Each of the five water distribution
206 pipe networks from DynaVIBe comprise the different samples for each city, because
207 they vary in their spatial distribution (Abdel-Mottaleb and Zhang 2019). Input for Dy-
208 naVibe includes digital elevation models, demand volume, and cyclicity percentage.
209 For each city, digital elevation models are downloaded from the Consortium for Spa-
210 tial Information database. For hydraulic consistency, a total demand of 1083.3 l/s is
211 used for all of the cities' network generation (as was used in previous studies since
212 Quindry et al. (1981)), and a constant cyclicity value of fifty percent is input. For a
213 given city and water network layout, the water distribution network is converted to a
214 shape file and imported into the ArcGIS user interface, and the transportation network
215 for the same city is also imported into GIS for geoprocessing.

216 **Interface Network Extraction and Model Construction**

217 After importing the two shape files (water distribution and transportation) into the
218 same ArcGIS map, a buffer is added to account for lane width (road lane information is
219 present in Openstreetmap GIS files). After adding the lane width buffer, both networks
220 are intersected using the intersect geoprocessing tool, resulting in a new feature layer
221 containing a subset of the original pipes and roads. After obtaining the intersect of the
222 overlaid pipe and road networks (shown in Figures 3 and 4), the interface network is
223 generated from the logical implications in the intersection: a pipe failure will cause
224 a road failure if it is below the road (or over a longer time, vehicular loads on roads
225 can stress water pipes). Thus, a node represents the pipe, another node represents
226 the road, and the causal link is represented by an edge between them. The attribute

227 table of the interface network consists of an edge list (i.e. a list of the edges, the
228 connections between water and transportation, where one column contains pipes, and
229 another contains the roads that are co-located to them), as shown in Figure 3. This
230 network represents unidirectional propagation of failure from the water distribution
231 pipes to the transportation roads in the event of a pipe failure. The attribute table is
232 exported as a spreadsheet for analysis in the following step.

FIG. 3

FIG. 4

233 **Network Analysis**

234 Classification of similar networks is challenging but using multiple measures for
235 comparison eases and enhances the accuracy of the process (Soundarajan et al. 2014).
236 There are network-wide measures representing facets of connectivity that are assumed
237 to indicate failure propagation, and there are nodal measures for each node in a given
238 network. Thus, two distinct network analyses are conducted: global, network-wide
239 and local, nodal-scale. An example of the distinction is the difference in measurement
240 scale between centralization and centrality; centrality refers to the nodal or component
241 scale (a micro-level measurement) whereas centralization is a global scale network-
242 wide metric (a macro-level measurement).

243 To conduct network analysis, the interface network for each city is imported as an
244 edge list into Cytoscape (an open source network analysis software by Doncheva et al.
245 (2012)). Within the software, the connected components of each network are automati-
246 cally identified. Because all of the tested interface networks contain a giant component
247 (containing >> 50 percent of the networks' nodes), only the giant component is used

248 in the analysis as is common in network analysis (Kolaczyk 2009). The network an-
249 alyzer and CytoCluster plugins are used to compute four network-wide connectivity
250 measures: modularity, heterogeneity, centralization, and average number of neighbors
251 (Doncheva et al. 2012; Li et al. 2017). Average number of neighbors is based on the
252 aggregate connectivity of network neighborhoods. It is calculated as the average of
253 the number of nodes that each node in the network is connected to. Centralization and
254 heterogeneity are closely related. Heterogeneity is the tendency of a network to con-
255 tain hub nodes. Similarly, centralization is the tendency of a network to have central
256 structure, meaning the presence of central nodes relative to how central other nodes
257 are in the network (Freeman et al. 1979). Thus, higher values of heterogeneity and
258 centralization indicate that connectivity is not homogeneous across the entire network.
259 Modularity examines connectivity from the vantage of community structure; it is the
260 strength of network division into communities. High modularity indicates high con-
261 nectivity between nodes in the same community or module, and sparser connections
262 between nodes of different modules.

263 The network analyzer plugin within Cytoscape is also used to compute the nodal at-
264 tributes: in-degree, out-degree, neighborhood connectivity, betweenness centrality, and
265 average shortest path length (Doncheva et al. 2012). The nodal degree is the number
266 of edges incident to a given node, meaning more connected nodes have higher in or
267 out degrees. Neighborhood connectivity is the mean of the number of neighbors for
268 all neighbors of a given node, and so higher values indicate higher nodal connectivity.
269 Betweenness centrality is the fraction of all shortest paths in the network that contain
270 a given node, while average shortest path length is the average length of all shortest
271 paths between a node and other nodes. The higher the betweenness centrality, the more
272 crucial a node is to the connectivity of a network (Freeman et al. 1979; Soundarajan
273 et al. 2014; Newman 2018). The shorter the average shortest path length of a node is,
274 the more highly connected it is.

275 Instead of using Cytoscape, the networkx package can be used within python for convenience.
276 After obtaining network wide measures, ANOVA and post hoc Tukey HSD
277 analyses are conducted to test if connectivity measures are statistically different among
278 cities using the Scikitlearn package in python, and to identify where the differences are
279 located.

280 **Clustering on Global Measures**

281 The hierarchical clustering of network-wide connectivity in this study is analyzed
282 to discern similar and different networks using a distance matrix based on four network-
283 wide connectivity measures. To eliminate the effects of scale on the analysis, connec-
284 tivity metrics are normalized prior to calculating a distance measurement between each
285 pair of measurements for all of the interface networks using dynamic time warping.
286 Dynamic time warping is a robust technique that is used in signal processing applica-
287 tions and other classification problems (Mueen and Keogh 2016). The mlpy (machine
288 learning python) was used for this method (Albanese et al. 2012).

289 Using the Scipy package within python, clustering was conducted to group cities' in-
290 terfaces based on the distance matrix of the global network-wide measures. A cluster-
291 ing criterion defines obtained clusters, imposing structure on the observations — it is
292 therefore important to evaluate whether the clusters do in fact group similar objects,
293 and distinct clusters are more different (Cesar Jr and da Fona Costa 2009). Ward's
294 linkage was used to cluster the cities' interfaces based on the network connectivity, be-
295 cause it is a dispersion-based clustering approach and is regarded as superior or the best
296 hierarchical clustering technique (Cesar Jr and da Fona Costa 2009). Though Ward's
297 linkage was used, other linkage techniques were tested and provided similar results.

298 **Roads Indegree Distribution**

299 In order to provide some physical understanding of information the interface net-
300 work provides, and to better demonstrate the data being input into the random forest

301 model, this study quantifies the indegree distribution of roads in the interface network.
302 The indegree distribution is the distribution of the number of roads with a given num-
303 ber of pipes intersecting them. This is an interesting property because irrespective of
304 type of mechanical failure of a pipe, the co-located road(s) must often be disturbed
305 as a consequence. The degrees of the transportation roads are extracted to identify
306 a best fit distribution, via methods explained in Clauset et al. (2009), using the net-
307 workx, matplotlib, scipy and numpy packages in python. The scaling parameters are
308 also determined as they reveal unique properties regarding the distributions' shape. In
309 particular, a power law distribution is tested for. If the distribution follows a power
310 law, $y = x^{-\alpha}$, then the scaling parameter, α , can provide insight about the hierarchy
311 of connections within the interface networks (e.g., is there a small proportion of roads
312 interacting with many pipes?).

313 **Random Forest Model and Feature Extraction**

314 Random forest is a powerful machine learning algorithm that uses a combination
315 of many decision trees (hence the name, forest) based on given predictors or classifiers
316 to make a prediction or classification. Using a training set, the model “learns” from
317 past data, and reduces the variance. It is of importance to ensure the diversity of the
318 input training set such that the random forest model is not biased. Due to the non-linear
319 and non-normal nodal network data, and the large number of samples, and multiplicity
320 of classifiers (i.e. the nodal features), a random forest model is used for nodal feature
321 extraction. The total samples for the random forest exceeded 1 million (nodes). The
322 large amount of data allowed for using fifty percent of the data for training the model.
323 The relative importance of a feature is measured by calculating the increase in the
324 model’s prediction error after shuffling the feature (Molnar 2019). A feature is impor-
325 tant in the model if shuffling its values increases the model error, because the model
326 relied on the feature for the prediction. If shuffling feature values leaves the model

327 error unchanged, then the model ignored the feature for the prediction, indicating the
328 feature is unimportant (Molnar 2019). This shuffling feature importance measurement
329 is described in Breiman et al. (1984) and in Breiman (2001) and Breiman (2002) for
330 random forests. It is called the “Gini importance” or “mean decrease impurity”, be-
331 cause it is a measure of the decrease in node impurity, averaged over all trees of the
332 ensemble (i.e. the random forest). The method is implemented in scikitlearn, the
333 python package used to calculate it for this study.

334 **RESULTS AND DISCUSSION**

335 **Measures of Connectivity**

336 For each interface sample, network-wide, global measures of connectivity are taken.
337 Figure 5 shows plots of the ANOVA with post-hoc Tukey HSD results for each city.
338 As shown in Figure 5, cities have statistically similar connectivity measures where the
339 bars overlap and where the bars do not overlap, they are statistically different with p
340 value ≤ 0.05 . From the plots shown in Figure 5, Rome and Portland appear at oppo-
341 site ends of the spectrum for each connectivity measure. It is also interesting to note
342 that values of sample centralization showed the highest variability among connectivity
343 measures, whereas the average number of neighbors showed the least variability. For
344 Heterogeneity, the samples for Dubai are between Rome, and Chicago and Atlanta.
345 Paris is between Chicago and Atlanta, and Boston and Alexandria. In terms of Modu-
346 larity, it was surprising that Rome’s samples were highest and Portland the lowest. Due
347 to the grid like shape of Portland’s infrastructure its individual physical infrastructures
348 (i.e., water distribution and transportation) appear to be more modular than those of
349 Rome. However, the grid-like pattern is no longer present in the interface network
350 when the connections between two infrastructures are examined. Just as surprising
351 is that Portland’s interface samples showed the highest centralization, whereas Rome,
352 Dubai, Chicago, and Atlanta have the lowest values for centralization. The centraliza-

tion values for Paris and Boston are higher, followed by Alexandria. It is interesting that Alexandria's samples are closer to Portland. Even though Alexandria is an older city, it is more coastal and has had newer expansion that may be cause for the similarity. The physical water and transportation infrastructures of Rome have centralization values three orders of magnitude higher than those of Portland (see Appendix), with higher connectivity in the center – so it is interesting that this characteristic does not translate to the interface network. Boston is between Rome and Portland, and the remaining cities were all more similar and closer in value to Rome than Portland. For the average number of neighbors, Alexandria's samples show the lowest values, and Portland's samples have the highest values. The value for Dubai's samples is between Alexandria's, and Rome, Paris, and Atlanta. Chicago's samples fall higher on the spectrum, and Boston's samples are between Chicago and Portland. This result signifies that characteristics of the physical infrastructures network are different from that of the logical interface network and not all cities have the same interface connectivity. As a result, clustering of the cities based on properties of the interface network is useful to investigate infrastructure interdependency and grouping them based on all four connectivity measures is necessary, because the similarities of cities' interface samples was not consistent across the four measures. For example, Alexandria was closer to Portland for two measures, but closer to Rome for the other two measures.

FIG. 5

372 Interface Connectivity Clusters

373 The results of the clustering analysis are shown in Figure 6. Two things are clear
374 from Figure 6. Cities can be clustered into three groups (in Figure 6, they correspond
375 to cluster 1 on the left (containing interface samples from Rome, Dubai, Chicago,
376 and Alexandria), cluster 2 in the middle (containing city samples from Alexandria,

Atlanta, and Paris), and cluster 3 on the right (containing city samples from Paris, Boston, and Portland)) based on the four measures of connectivity used in the analysis of variance. The three clusters are selected for two reasons: to maximize the distance (i.e. ensure that distinct cluster labels are actually different from each other), and to ensure that the distances obtained from a clustering technique accurately reflect the original data. This is often checked using the cophenetic correlation coefficient, introduced in Sokal and Rohlf (1962). It measures the linear correlation coefficient between dissimilarity between each pair of observations (i.e. original connectivity data) and their cophenetic distance (i.e. the vertical distances between where clusters diverge shown in the dendrogram). The cut dendrogram does have a cophenetic correlation coefficient ≥ 0.75 , indicating that the clustering technique accurately represents the data. A few cities' samples (e.g., Alexandria and Paris) are divided between two different clusters. These two cities have a higher variability in their resulting interface network based on the input water distribution configuration. This observation indicates individual infrastructure system design and subsequent layout are driving forces of a city's interface network properties. Consequentially, engineers and urban planners may influence failure propagation from water infrastructure by accounting for a city's interface connectivity when designing water distribution systems. It also appears that cities with similar geospatial morphology tend to cluster together; Alexandria and Rome are closer to each other than they are to Portland. Portland, being the most grid-like shaped city, is closer to more grid-like cities such as Boston. Similarly, Rome, an older, circular city is clustered closer to Chicago which is one of the cities that has previously been identified to be modeled after older European cities in Louf and Barthelemy (2014). Rome, Dubai, Chicago, and Alexandria are clustered together, and are categorized under Cluster 1. Cluster 2 includes Alexandria, Atlanta, and Paris, and Cluster 3 includes: Paris, Boston, and Portland. Thus, for the nodal network measures, each node is labelled with either connectivity cluster 1, 2, or 3 depending on which

connectivity cluster its sample is a part of, enabling use of random forest.

FIG. 6

404

405 **Road Indegree Distribution**

406 In Figure 7, one of the studied nodal attributes (Indegree) that are used in conjunc-
407 tion with the clusters for constructing the model is shown in detail. The significant
408 power law distribution of indegrees for all of the tested interface networks indicates
409 that there are some roads with very high connectivity to water distribution pipes, while
410 most roads are not as highly connected to water pipes. Roads with higher indegree
411 tend to be “secondary”, connecting main highways to the neighborhoods. The power
412 law distribution confirms this physical pretext, that has already been demonstrated for
413 water distribution networks (Zischg et al. 2017). But the scaling parameter, the power
414 law exponent, provides nuance. It is significant within the random forest model (as
415 determined from the feature extraction), suggesting the hierarchy of the infrastructure
416 as guided by urban development is an important factor in determining interface con-
417 nectivity. Hierarchy here is quantified by the power law exponent, because the larger
418 its magnitude, the more gradual the indegree distribution falls. The smaller the expo-
419 nent magnitude is, the more unevenly distributed the pipe-road connectivity is among
420 the roads, and the less “balanced the interdependency is”. For example, Rome has the
421 largest magnitude of the power law exponent ($\alpha = 2.4$), and Portland has the smallest
422 magnitude ($\alpha = 0.95$). This is interesting as Rome and Portland are very different
423 in their spatial layout as shown in their polar histograms in Figure 2, where Rome is
424 most circular, and Portland is most grid-like. Another observation is that for all of
425 the interface networks, the power-law tail begins at an indegree equal or larger than
426 10 pipes. This means that the power law relationship holds strongest for roads with
427 greater than 10 pipes intersecting them at some location. The characterization of the

428 power law exponents implicitly denotes the relationship between the road size/capacity
429 and their corresponding connectivity to water pipes. A less evenly distributed hierarchy
430 of connections between water pipes and transportation roads (i.e. lower value scaling
431 parameter) suggests that it is possible for large road failures to be induced by seemingly
432 inconsequential failures in the water distribution network. This result would be con-
433 sistent with the findings regarding urban drainage and transportation from Wang et al.
434 (2019), that localized floods can induce catastrophic road failures for some networks.

FIG. 7

435 **Random Forest Model Prediction**

436 From the random forest model, it is determined that, with 90 percent accuracy, a
437 node's connectivity cluster can be predicted using the input nodal features (between-
438 ness centrality, in-degree, out-degree, average shortest path length, and neighborhood
439 centrality). A confusion matrix contains information pertinent to the accuracy of the
440 model in identifying a connectivity cluster of nodes from nodal properties. The con-
441 fusion matrix shown in Figure 8 contains more detail on the distribution of model
442 accuracy in distinguishing different clusters from each other. The x-axis of the ma-
443 trix represents the predicted city connectivity cluster of a sample by the random forest
444 model. The y-axis represents the actual city connectivity cluster. The matrix is read
445 by row, and the diagonal represents the normalized number of samples accurately clas-
446 sified (actual cluster matches the predicted cluster) by the random forest model. The
447 diagonal in Figure 8 has the highest number of normalized number of samples owing
448 to the high accuracy of the model. The matrix also indicates that the accuracy in iden-
449 tifying samples from clusters 1 and 3 is higher than identifying samples from cluster
450 2. It can also be observed from the 90 percent accuracy that nodal properties can pre-
451 dict a given connectivity cluster; this relates to the micro-nodal scale measures being

452 able to predict global network-wide patterns. The random forest also enables feature
453 extraction of the nodal property contributing the most to the prediction/classification,
454 by shuffling attributes and evaluating the change in model accuracy.

FIG. 8

455 **Feature Extraction**

456 From the feature extraction, for which results are shown in Figure 9, average short-
457 est path length accounts for 60 percent of the relative importance in the identifica-
458 tion/prediction of the connectivity cluster a given node belongs to. This is much
459 higher than any other nodal attributes. Average shortest path length has previously
460 been shown to correlate with an individual water distribution network's performance.
461 Specifically, for individual water distribution networks, average shortest path length
462 positively correlates to redundancy and consequently network resilience (Giudicianni
463 et al. 2018). This research extends the predicative utility of average shortest path length
464 of nodes from single infrastructure networks to predict connectivity between interface
465 networks of coupled, co-located infrastructures.

FIG. 9

466 **CONCLUSION**

467 In this work, we conclude that interface networks representing potential failure
468 propagation from water distribution to transportation infrastructures may differ in their
469 network connectivity depending on the water distribution layout for a given transporta-
470 tion network in a city. Practically, WDN design, despite the WDN being co-located,
471 still has sufficient leverage to alter the connectivity profile of the interface between
472 road and water. This indicates that the location/structure of redundancies in a WDN

473 can significantly influence co-location (and thus propagation of failure from one in-
474 frastructure to another), as seen for two of the studied cities.

475 The variation in connectivity allowed the clustering of city interface networks based
476 on connectivity. Further, the study determined that nodal properties, such as neighbor-
477 hood connectivity and average shortest path length, can predict the connectivity cluster
478 of an interface network that a given node belongs to. The study finds average shortest
479 path length to be the most powerful attribute in predicting connectivity. Future work
480 can validate connectivity clusters with simulation performance data and formulate an
481 optimization model to minimize the failure propagation by changing interface network
482 layouts using extracted nodal feature(s).

483 The study also found that the directional connectivity of water pipes to roads for the
484 studied cities follows a power law, but with varying scaling or hierarchy. These in-
485 sights are a step at answering 1) how to mathematically represent connectivity of the
486 coupled interface structure and 2) how much does a given urban development pattern
487 influence the connectivity of water-transportation interfaces. Such understanding can
488 have practical implications in terms of designing the desired interfaces by modifying
489 both urban form/development and some aspects of water distribution networks so that
490 a lower failure propagation can be achieved from a water distribution network to a
491 co-located road network. Future work will investigate network layouts with lower in-
492 terface connectivity, as that is assumed to propagate less failure from water distribution
493 to transportation infrastructure.

494 The interdependency between urban water distribution and transportation networks is
495 doubtlessly present, but the extent is not fully understood nor quantified; hence, char-
496 acterizing the interdependencies between urban water distribution and transportation
497 systems can aid in the optimization of both networks by informing design, operations
498 and maintenance.

499

DATA AVAILABILITY STATEMENT

500

501

502

503

504

505

506

507

- Some or all data, models, or code generated or used during the study are available in a repository online in accordance with funder data retention policies (“Water distribution–transportation interface network data”, DOI: 10.5281/zenodo.3381596)
- All data, models, or code generated or used during the study are available from the corresponding author by request (generated interface networks, analysis of variance, clustering, random forest, and feature extraction).

ACKNOWLEDGEMENTS

508

509

510

511

512

This material is based upon work supported by the National Science Foundation under Grant Number 1638301. Any opinions, findings, and conclusions or recommendations expressed in this material are those of the authors and do not necessarily reflect the views of the National Science Foundation. Preliminary results were orally presented at the AWRA GISX Conference in Orlando, FL (April, 2018).

513 REFERENCES

514 Abdel-Mottaleb, N., Ghasemi Saghand, P., Charkhgard, H., and Zhang, Q. (2019).
515 “An exact multiobjective optimization approach for evaluating water distribution in-
516 frastructure criticality and geospatial interdependence.” *Water Resources Research*,
517 55(7), 5255–5276.

518 Abdel-Mottaleb, N. and Zhang, Q. (2019). “Water distribution–transportation interface
519 network data, <DOI: 10.5281/zenodo.3381596>.

520 Agafonkin, V. (2018). “Visualizing street orientations on an interactive map,
521 <<https://mourner.github.io/road-orientation-map/>>.

522 Ahern, J. (2011). “From fail-safe to safe-to-fail: Sustainability and resilience in the
523 new urban world.” *Landscape and urban Planning*, 100(4), 341–343.

524 Albanese, D., Visintainer, R., Merler, S., Riccadonna, S., Jurman, G., and Furlanello,
525 C. (2012). “mlpy: Machine learning python.” *arXiv preprint arXiv:1202.6548*.

526 Alexander, C. (1977). *A pattern language: towns, buildings, construction*. Oxford uni-
527 versity press.

528 Bianconi, G. (2018). *Multilayer Networks: Structure and Function*. Oxford university
529 press.

530 Boccaletti, S., Bianconi, G., Criado, R., Del Genio, C. I., Gómez-Gardenes, J., Ro-
531 mance, M., Sendina-Nadal, I., Wang, Z., and Zanin, M. (2014). “The structure and
532 dynamics of multilayer networks.” *Physics Reports*, 544(1), 1–122.

533 Boeing, G. (2017). “Methods and measures for analyzing complex street networks and
534 urban form.” *arXiv preprint arXiv:1708.00845*.

535 Boeing, G. (2019). “Urban spatial order: Street network orientation, configuration, and
536 entropy.” *Configuration, and Entropy (February 1, 2019)*.

537 Breiman, L. (2001). “Random forests.” *Machine learning*, 45(1), 5–32.

538 Breiman, L. (2002). “Manual on setting up, using, and understanding random forests
539 v3. 1.” *Statistics Department University of California Berkeley, CA, USA*, 1, 58.

540 Breiman, L., Friedman, J., Olshen, R., and Stone, C. (1984). “Classification and re-
541 gression trees. wadsworth int.” *Group*, 37(15), 237–251.

542 Buldyrev, S. V., Parshani, R., Paul, G., Stanley, H. E., and Havlin, S. (2010). “Cata-
543 strophic cascade of failures in interdependent networks.” *Nature*, 464(7291), 1025.

544 Casalicchio, E. and Galli, E. (2008). “Metrics for quantifying interdependencies.” *In-
545 ternational Conference on Critical Infrastructure Protection*, Springer, 215–227.

546 Cesar Jr, R. M. and da Fona Costa, L. (2009). *Shape classification and analysis: theory
547 and practice*. Crc Press.

548 Chen, A., Evans, B., Prior, A., Djordjevic, S., Savic, D., Butler, D., Goodey, P.,
549 Stevens, J. R., and Colclough, G. (2018). “Mapping urban infrastructure interde-
550 pendencies and fuzzy risks.

551 Clauset, A., Shalizi, C. R., and Newman, M. E. (2009). “Power-law distributions in
552 empirical data.” *SIAM review*, 51(4), 661–703.

553 Contributors, O. (2012). “Openstreetmap.” *URL www. openstreetmap. org*.

554 Danziger, M. M., Shekhtman, L. M., Bashan, A., Berezin, Y., and Havlin, S. (2016).
555 *Vulnerability of interdependent networks and networks of networks*. Springer.

556 Das, A., Banerjee, J., and Sen, A. (2014). “Root cause analysis of failures in inter-
557 dependent power-communication networks.” *Military Communications Conference
(MILCOM), 2014 IEEE*, IEEE, 910–915.

559 Di Nardo, A., Di Natale, M., Giudicianni, C., Greco, R., and Santonastaso, G. F.
560 (2018). “Complex network and fractal theory for the assessment of water distri-
561 bution network resilience to pipe failures.” *Water Science and Technology: Water
562 Supply*, 18(3), 767–777.

563 Doncheva, N. T., Assenov, Y., Domingues, F. S., and Albrecht, M. (2012). “Topolog-
564 ical analysis and interactive visualization of biological networks and protein struc-
565 tures.” *Nature protocols*, 7(4), 670.

566 Dueñas-Osorio, L., Craig, J. I., Goodno, B. J., and Bostrom, A. (2007). “Interdepen-

567 dent response of networked systems.” *Journal of Infrastructure Systems*, 13(3), 185–
568 194.

569 Freeman, L. C., Roeder, D., and Mulholland, R. R. (1979). “Centrality in social net-
570 works: II. experimental results.” *Social networks*, 2(2), 119–141.

571 Gastner, M. T. and Newman, M. E. (2004). “Diffusion-based method for produc-
572 ing density-equalizing maps.” *Proceedings of the National Academy of Sciences*,
573 101(20), 7499–7504.

574 Gillette, J., Fisher, R., Peerenboom, J., and Whitfield, R. (2002). “Analyzing wa-
575 ter/wastewater infrastructure interdependencies..” *Report no.*, Argonne National
576 Lab., IL (US).

577 Giudicianni, C., Di Nardo, A., Di Natale, M., Greco, R., Santonastaso, G., and Scala,
578 A. (2018). “Topological taxonomy of water distribution networks. water 10 (4): 1–
579 19.

580 Giustolisi, O., Simone, A., and Ridolfi, L. (2017). “Network structure classification
581 and features of water distribution systems.” *Water Resources Research*, 53(4), 3407–
582 3423.

583 Guidotti, R., Chmielewski, H., Unnikrishnan, V., Gardoni, P., McAllister, T., and
584 van de Lindt, J. (2016). “Modeling the resilience of critical infrastructure: The role
585 of network dependencies.” *Sustainable and resilient infrastructure*, 1(3-4), 153–168.

586 Haimes, Y. Y., Horowitz, B. M., Lambert, J. H., Santos, J. R., Lian, C., and Crowther,
587 K. G. (2005). “Inoperability input-output model for interdependent infrastructure
588 sectors. i: Theory and methodology.” *Journal of Infrastructure Systems*, 11(2), 67–
589 79.

590 Johansen, C. and Tien, I. (2018). “Probabilistic multi-scale modeling of interdependen-
591 cies between critical infrastructure systems for resilience.” *Sustainable and Resilient
592 Infrastructure*, 3(1), 1–15.

593 Kivelä, M., Arenas, A., Barthelemy, M., Gleeson, J. P., Moreno, Y., and Porter, M. A.

594 (2014). “Multilayer networks.” *Journal of complex networks*, 2(3), 203–271.

595 Kolaczyk, E. D. (2009). *Statistical Analysis of Network Data: Methods and Models*
596 (01).

597 Korkali, M., Veneman, J. G., Tivnan, B. F., Bagrow, J. P., and Hines, P. D. (2017). “Re-
598 ducing cascading failure risk by increasing infrastructure network interdependence.”
599 *Scientific reports*, 7, 44499.

600 Li, M., Li, D., Tang, Y., Wu, F., and Wang, J. (2017). “Cytocluster: A cytoscapeplugin
601 for cluster analysis and visualization of biological networks.” *International journal*
602 *of molecular sciences*, 18(9), 1880.

603 Louf, R. and Barthelemy, M. (2014). “A typology of street patterns.” *Journal of The*
604 *Royal Society Interface*, 11(101), 20140924.

605 Mair, M., Zischg, J., Rauch, W., and Sitzenfrei, R. (2017). “Where to find water pipes
606 and sewers??on the correlation of infrastructure networks in the urban environment.”
607 *Water*, 9(2), 146.

608 Mapbox, L. (2018). “Mapbox studio, <<https://www.mapbox.com/mapbox-studio/>>.”

609 Meerow, S., Newell, J. P., and Stults, M. (2016). “Defining urban resilience: A review.”
610 *Landscape and urban planning*, 147, 38–49.

611 Molnar, C. (2019). *InterpretableMachineLearning*,
612 <<https://christophm.github.io/interpretable-ml-book/>>.

613 Mueen, A. and Keogh, E. (2016). “Extracting optimal performance from dynamic
614 time warping.” *Proceedings of the 22nd ACM SIGKDD International Conference*
615 *on Knowledge Discovery and Data Mining*, ACM, 2129–2130.

616 Newman, M. (2018). *Networks*. Oxford university press.

617 Ouyang, M. (2014). “Review on modeling and simulation of interdependent critical
618 infrastructure systems.” *Reliability engineering & System safety*, 121, 43–60.

619 Ouyang, M. and Dueñas-Osorio, L. (2011a). “An approach to design interface topolo-
620 gies across interdependent urban infrastructure systems.” *Reliability Engineering &*

621 *System Safety*, 96(11), 1462–1473.

622 Ouyang, M. and Dueñas-Osorio, L. (2011b). “Efficient approach to compute general-
623 ized interdependent effects between infrastructure systems.” *Journal of Computing*
624 in *Civil Engineering*, 25(5), 394–406.

625 Ouyang, M., Dueñas-Osorio, L., and Min, X. (2012). “A three-stage resilience analysis
626 framework for urban infrastructure systems.” *Structural safety*, 36, 23–31.

627 Porta, S., Crucitti, P., and Latora, V. (2006). “The network analysis of urban streets: a
628 primal approach.” *Environment and Planning B: planning and design*, 33(5), 705–
629 725.

630 Quindry, G. E., Liebman, J. C., and Brill, E. D. (1981). “Optimization of looped water
631 distribution systems.” *Journal of the Environmental Engineering Division*, 107(4),
632 665–679.

633 Rahnamay-Naeini, M. and Hayat, M. M. (2016). “Cascading failures in interdependent
634 infrastructures: An interdependent markov-chain approach.” *IEEE Transactions on*
635 *Smart Grid*, 7(4), 1997–2006.

636 Reed, D. (2017). *Water, Security and US Foreign Policy*. Taylor & Francis.

637 Rinaldi, S. M., Peerenboom, J. P., and Kelly, T. K. (2001). “Identifying, understand-
638 ing, and analyzing critical infrastructure interdependencies.” *IEEE control systems*
639 *magazine*, 21(6), 11–25.

640 Sitzenfrei, R., Fach, S., Kleidorfer, M., Urich, C., and Rauch, W. (2010). “Dynamic vir-
641 tual infrastructure benchmarking: Dynavibe.” *Water Science & Technology*, 10(4),
642 600.

643 Sokal, R. R. and Rohlf, F. J. (1962). “The comparison of dendograms by objective
644 methods.” *Taxon*, 11(2), 33–40.

645 Soundarajan, S., Eliassi-Rad, T., and Gallagher, B. (2014). “A guide to selecting a net-
646 work similarity method.” *Proceedings of the 2014 SIAM International Conference*
647 on *Data Mining*, SIAM, 1037–1045.

648 Svendsen, N. K. and Wolthusen, S. D. (2007). “Connectivity models of interdepen-
649 dency in mixed-type critical infrastructure networks.” *Information Security Techni-*
650 *cal Report*, 12(1), 44–55.

651 Wang, W., Yang, S., Stanley, H. E., and Gao, J. (2019). “Local floods induce large-
652 scale abrupt failures of road networks.” *Nature communications*, 10(1), 2114.

653 Winkler, J., Dueñas-Osorio, L., Stein, R., and Subramanian, D. (2011). “Interface net-
654 work models for complex urban infrastructure systems.” *Journal of Infrastructure*
655 *Systems*, 17(4), 138–150.

656 Yang, S., Paik, K., McGrath, G. S., Urich, C., Krueger, E., Kumar, P., and Rao, P.
657 S. C. (2017). “Functional topology of evolving urban drainage networks.” *Water*
658 *Resources Research*, 53(11), 8966–8979.

659 Yazdani, A. and Jeffrey, P. (2010). “A complex network approach to robustness and
660 vulnerability of spatially organized water distribution networks.” *arXiv preprint*
661 *arXiv:1008.1770*.

662 Yazdani, A. and Jeffrey, P. (2012). “Water distribution system vulnerability analysis
663 using weighted and directed network models.” *Water Resources Research*, 48(6).

664 Zhang, X., Miller-Hooks, E., and Denny, K. (2015). “Assessing the role of network
665 topology in transportation network resilience.” *Journal of Transport Geography*, 46,
666 35–45.

667 Zischg, J., Klinkhamer, C., Zhan, X., Krueger, E., Ukkusuri, S., Rao, P., Rauch, W.,
668 and Sitzenfrei, R. (2017). “Evolution of complex network topologies in urban water
669 infrastructure.” *World Environmental and Water Resources Congress 2017*, 648–
670 659.

671 **APPENDIX I. CENTRALIZATION AND ROAD INDEGREE DATA**

672 The centralization of Rome's individual infrastructure networks is $3.5 * 10^{-5}$. The
673 centralization of Portland's individual infrastructure networks is $2.0 * 10^{-8}$. In con-
674 trast, the centralization of Portland's interface network is higher than that of Rome's
675 interface network. These values are obtained using networkx within python. Cen-
676 tralization is normalized by the maximum possible centralization for a graph with the
677 same number of nodes (i.e. a star configuration). It is not surprising that the physical
678 infrastructure networks of Rome would have higher centralization values than Portland
679 because Rome's layout more closely resembles a star while Portland's layout resem-
680 bles a grid. For more on centralization, see Freeman (1979) and Newman (2018).

681 Figure 8 shows the road indegree distributions for the studied cities. Table 1 contains
682 more information regarding the cities' road indegree distributions (values of the scaling
683 parameter (α), and p-values).

TABLE 1: Power Law Data for Road Indegree Distributions

City	α range	p-value range
Alexandria	[1.43, 1.53]	$[10^{-17}, 10^{-13}]$
Atlanta	[1.80, 1.88]	$[10^{-26}, 10^{-22}]$
Boston	[1.28, 1.33]	$[10^{-33}, 10^{-30}]$
Chicago	[1.88, 1.96]	$[10^{-52}, 10^{-48}]$
Dubai	[2.01, 2.14]	$[10^{-16}, 10^{-14}]$
Paris	[1.77, 1.84]	$[10^{-24}, 10^{-23}]$
Portland	[0.93, 0.98]	$[10^{-22}, 10^{-21}]$
Rome	[2.39, 2.48]	$[10^{-19}, 10^{-16}]$

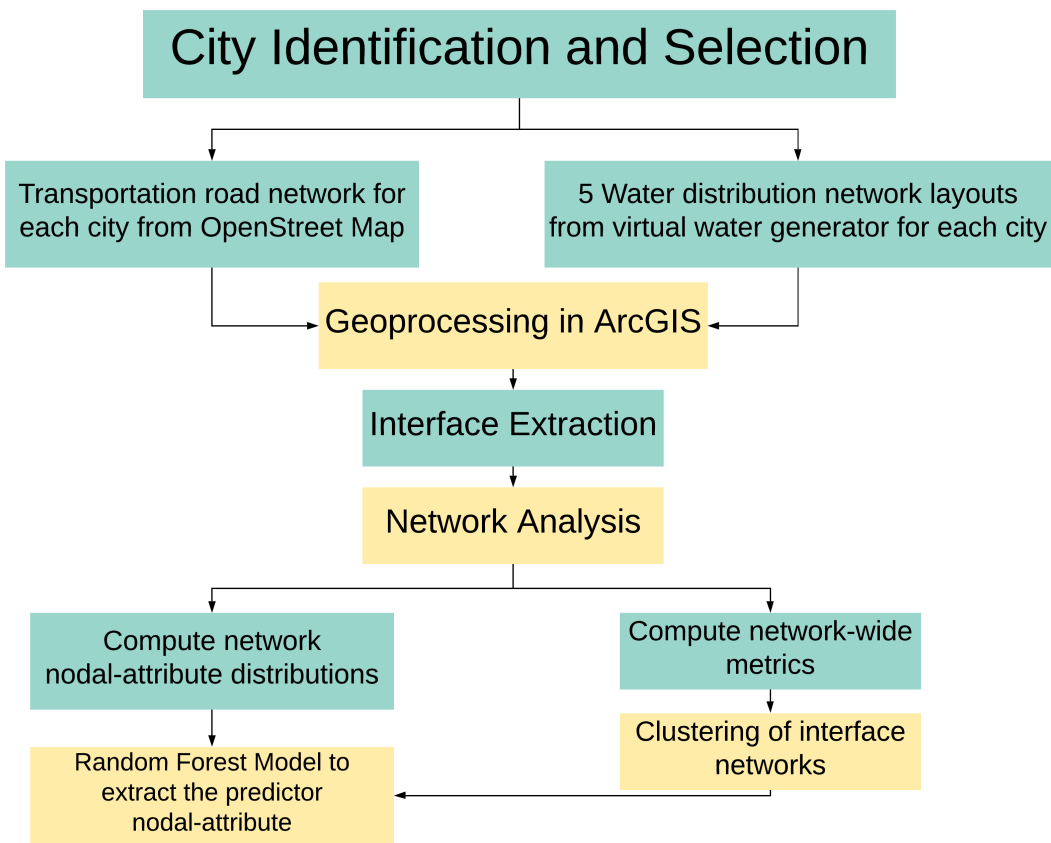


FIG. 1: Flowchart of study methodology starting with the city selection and ending with the extraction of a predictor nodal attribute

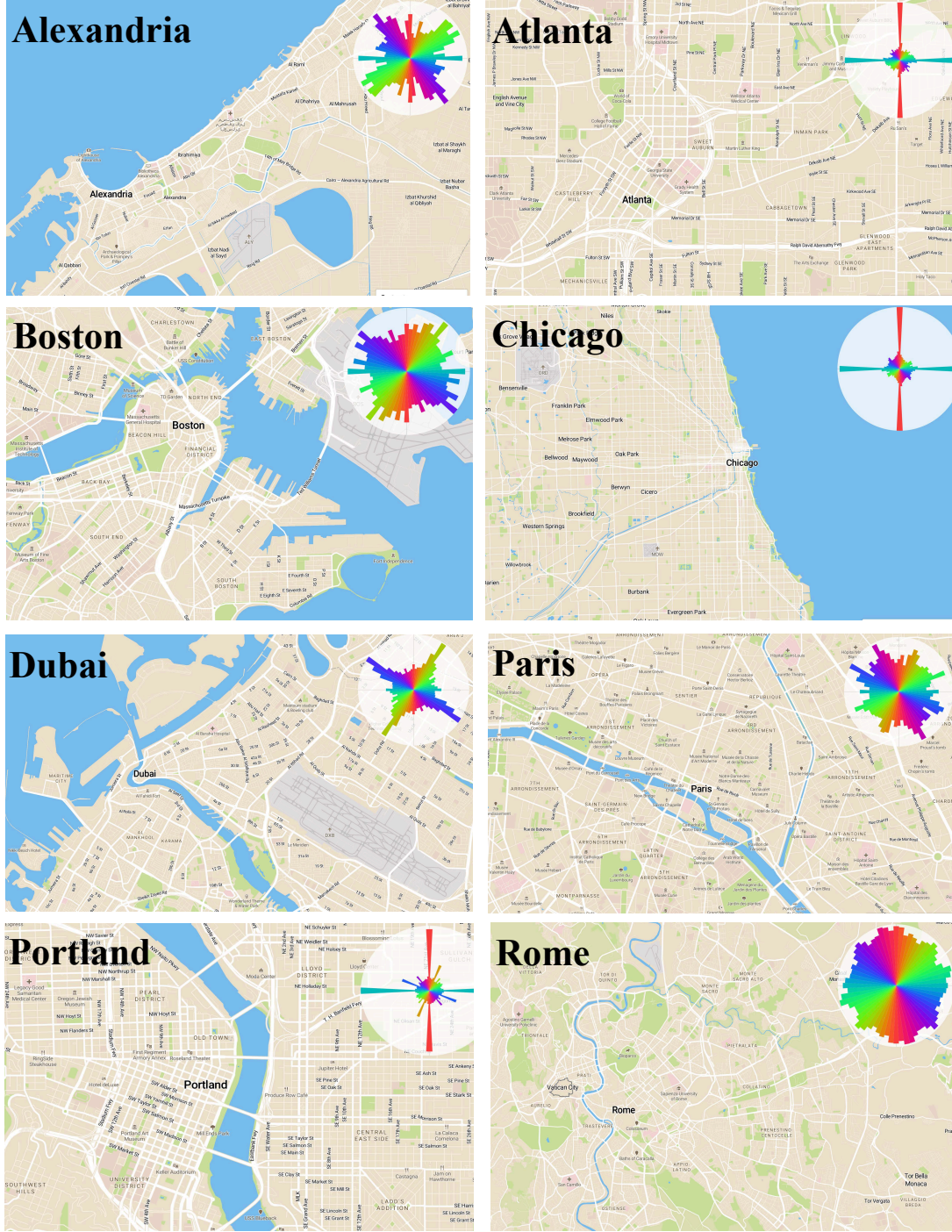


FIG. 2: Maps of the studied cities, with inlaid polar histograms representing the proportions of streets in different directions for each city. Portland is the most grid-like (polar histograms showing the majority of roads are along four directions). Rome is the most circularly developed city (polar histogram showing roads in about equal proportions lie in every direction).

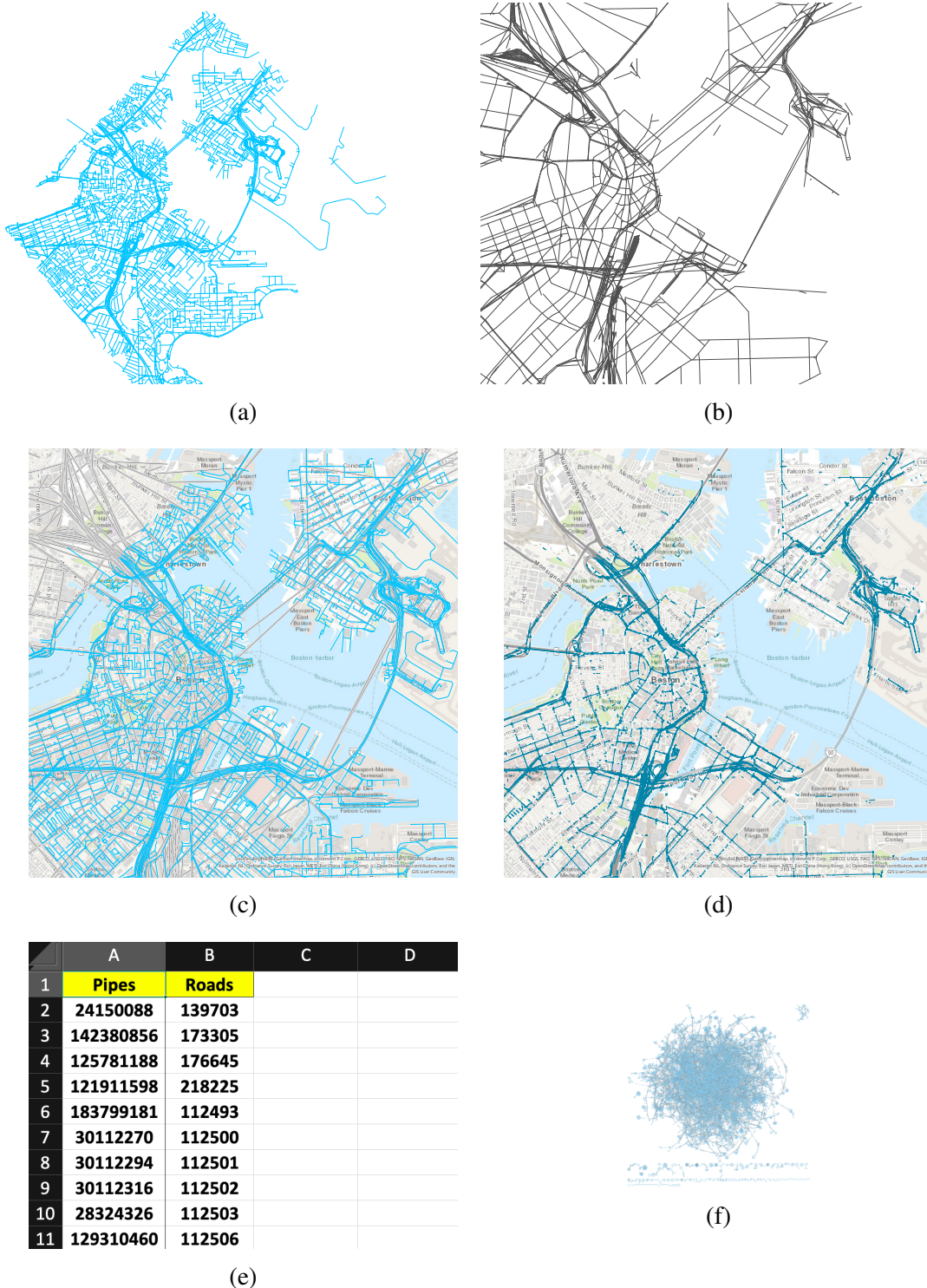


FIG. 3: (a) A Boston water network sample (b) Boston road network (c) Overlay of water and road Networks (d) Physical representation of interface (i.e. co-located pipes and roads) (e) The edgelist of pipes and roads that is imported into cytoscape (f) Interface network representation in cytoscape, giant connected component can be seen in the center (no longer spatially embedded), and much smaller disconnected components are also shown



FIG. 4: Pipe and road intersections: one sample map of each city's intersection of pipes and roads. The interface networks are constructed from these intersections, where each line or point on the map represents a connection between a pipe and road.

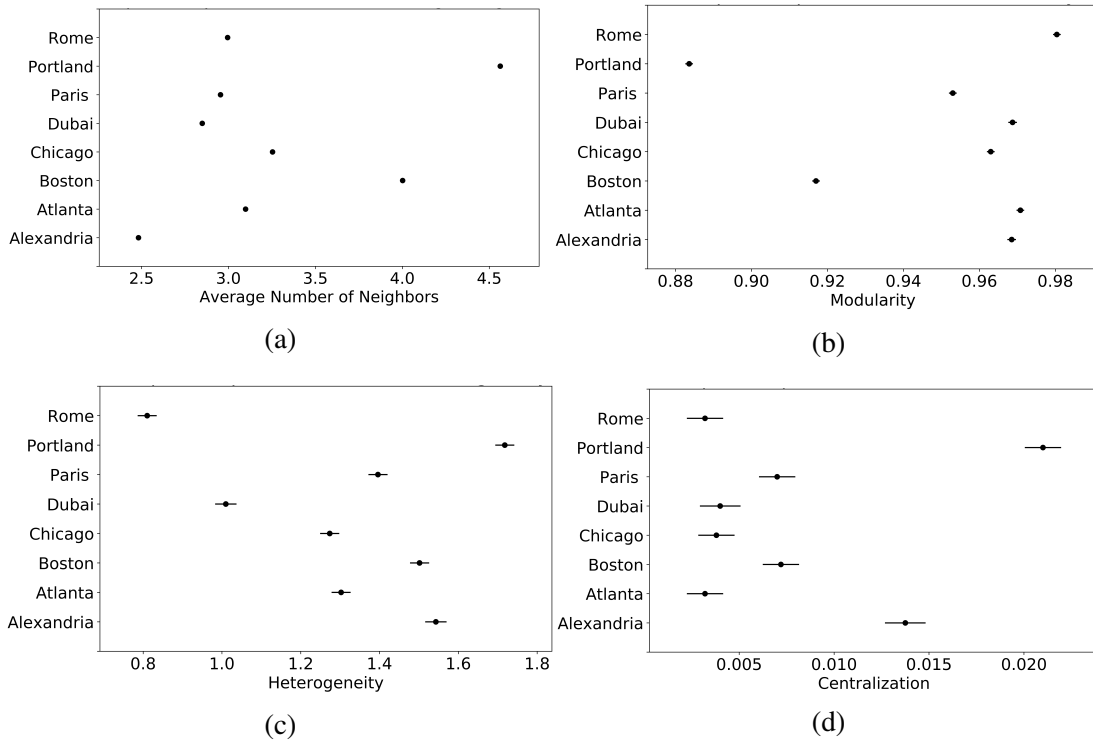


FIG. 5: Plots of the multiple comparison of means for the network-wide connectivity metrics: the x-axes are values of the different connectivity metrics (a) average number of neighbors (b) modularity (c) heterogeneity (d) centralization; the y-axes contain the different cities; each horizontal bar is summarizing the confidence intervals for the 5 samples of a given city; the plots show results from the multiple comparison of means from the post-hoc analysis for each connectivity measure; if the horizontal bars (of different city samples) in a plot overlap, the cities' interface network samples are not statistically different, but if they are not overlapping at all, then they are significantly different with $p\text{-value} \leq 0.05$.

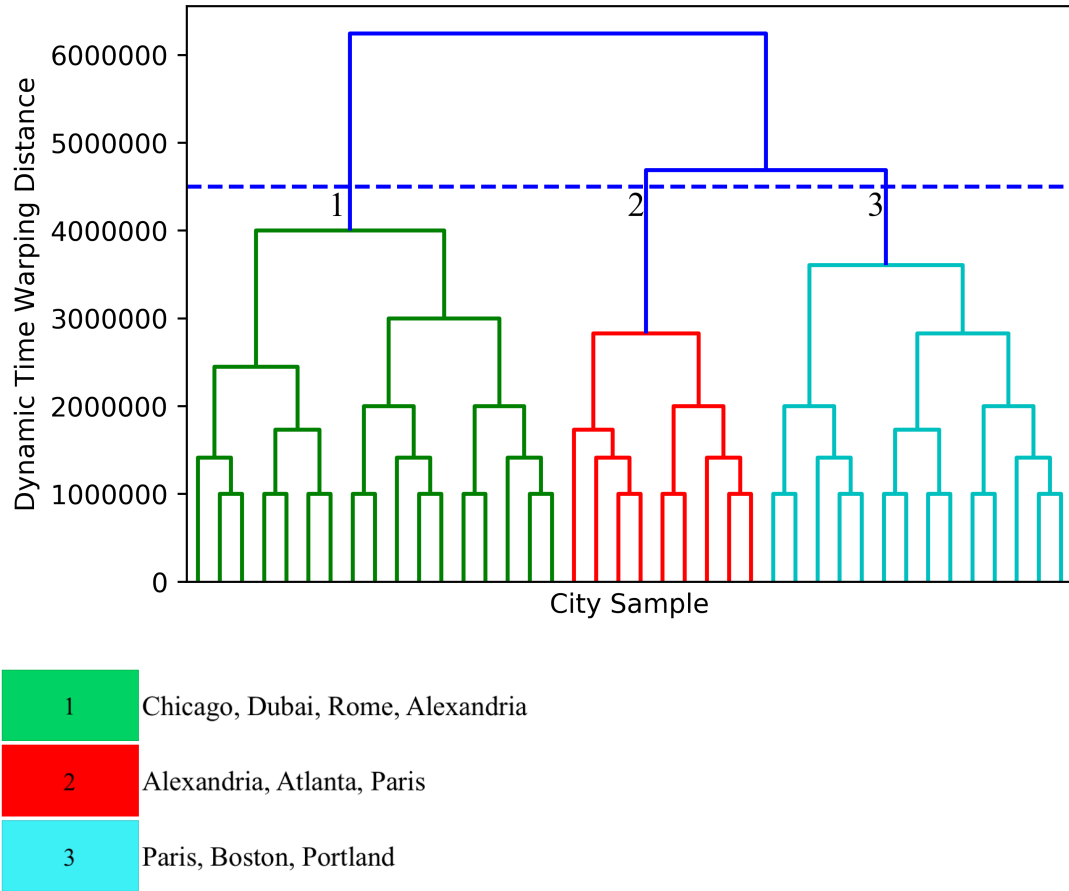


FIG. 6: Dendrogram of interface network connectivity: Along the x-axis are different city samples; The y-axis represents the distance between samples and their clusters, the lower the distance of the horizontal line connecting two samples or clusters, the more similar they are to each other; the further the distance at which two clusters are connected with a horizontal line, the more dissimilar they are. The dashed line intersecting the dendrogram is the location of the “cut” based on the two criteria for identifying clusters. As a result, three clusters are identified (1, 2, and 3), highlighted in different color.

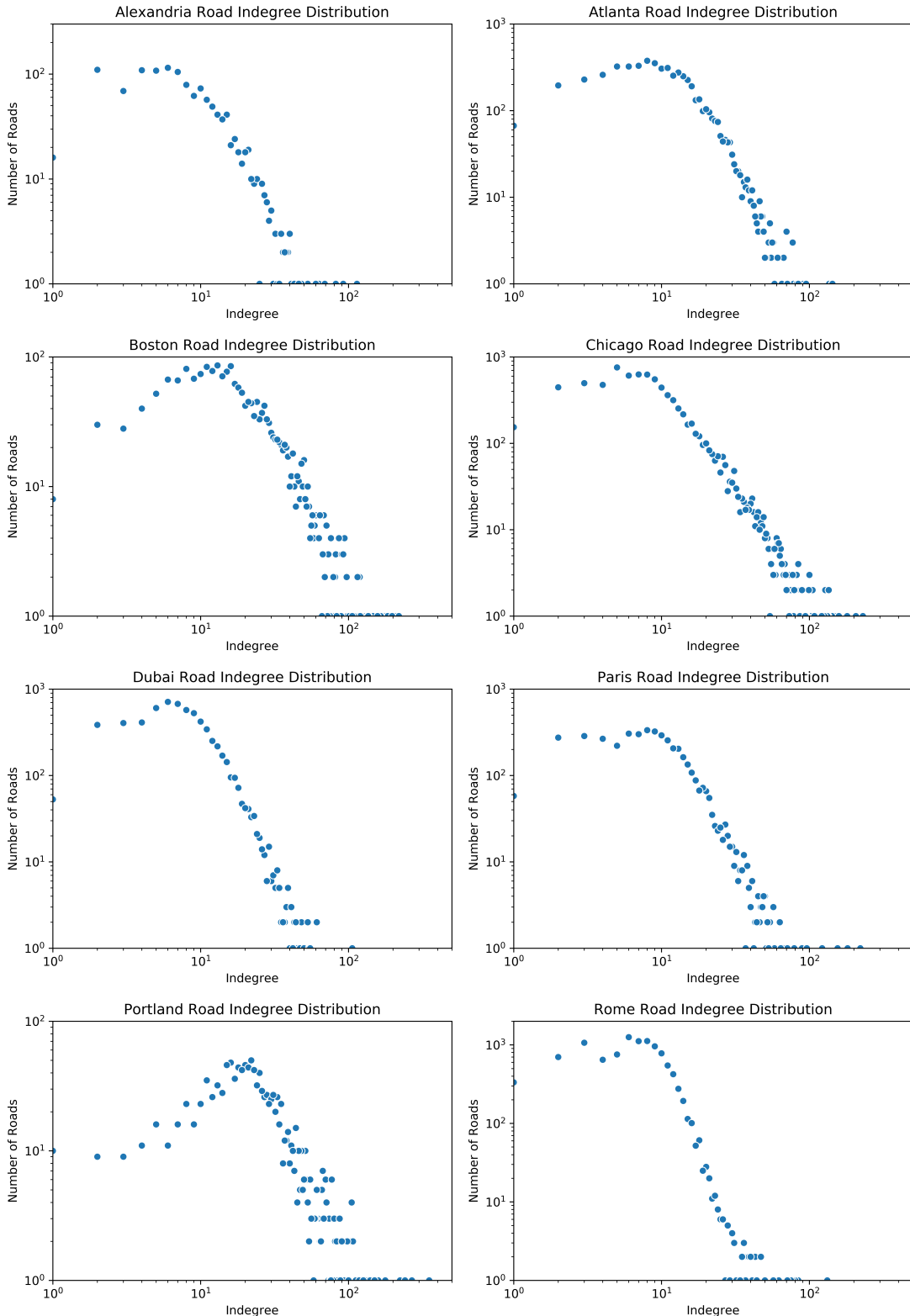


FIG. 7: Indegree distribution of roads in the interface networks for the studied cities. Axes are plotted on a log-log scale. The x-axis of these plots represents the number of pipes that intersect a road, this is the “indegree” of a given road. The y-axis represents the frequency, or number of roads, for which a given indegree occurs. Significant power-law tail is evident for all distributions at the same indegree value of 10, because of the linearity on the log-log scale.

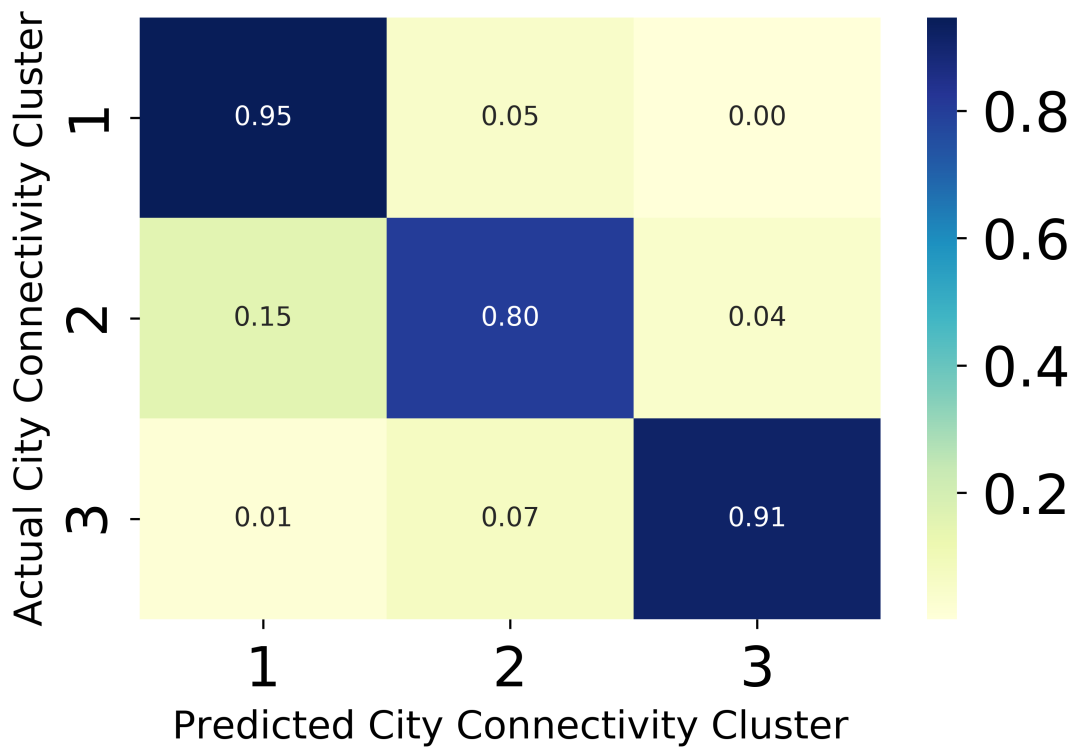


FIG. 8: Random forest model confusion matrix: The x-axis contains the city connectivity clusters predicted by the model; the y-axis contains the actual city connectivity clusters. The matrix is read by row, where values are the normalized number of samples predicted for each cluster. The values along the diagonal represent accuracies because the actual and predicted clusters are the same.

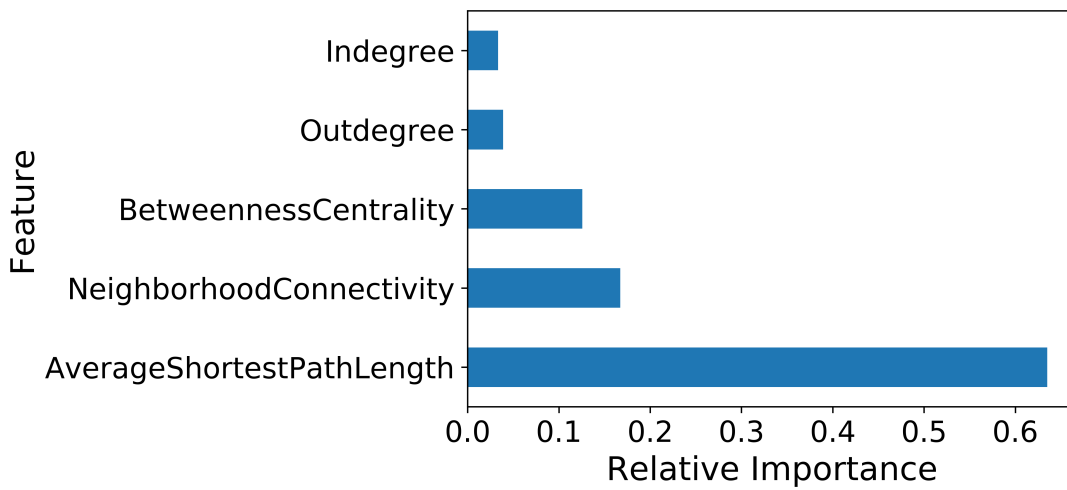


FIG. 9: Relative importance of nodal attributes to the prediction of the network-wide connectivity cluster by the random forest model: Average shortest path length is the most important nodal-attribute for the model in distinguishing between clusters.